J Mol Model (2017) 23: 15
DOI 10.1007/s00894-016-3187-6

ORIGINAL PAPER

Interactions of calcium with the external surfaces of fullerenes and endofullerenes doped with radioactive sodium iodide

Alejandro Valderrama[1] · **Radamés Reynoso**[1] · **Raúl W. Gómez**[1] · **Vivianne Marquina**[1] · **Martín Romero**[1]

Received: 22 August 2016 / Accepted: 6 December 2016 / Published online: 29 December 2016
© Springer-Verlag Berlin Heidelberg 2016

Abstract We report first-principles calculations carried out to analyze the adsorption of calcium on the outer surface of the fullerene C_{60}, yielding [$C_{60} + m$Ca]. Geometric optimization (GO) and molecular dynamics (MD) simulation were performed using the plane-wave pseudopotential method within the framework of density functional theory (DFT) and time-dependent DFT (TD-DFT) to investigate the configurations, the associated energies in the ground state, and the stabilities of fullerenes and endofullerenes doped with radioactive sodium iodide when they interact with calcium atoms on the outer fullerene surface (i.e., [nNa^{131}I@$C_{60} + m$Ca]). The reason for investigating these calcium-functionalized (endo)fullerene systems was to gauge their potential stability when used as vectors to deliver radioiodine to cancerous tissue in the human body. In the simulations, we found that the geometric limit on the number of calcium atoms that can be physisorbed on the outer surface of an empty fullerene while maintaining its structural stability is 28 calcium atoms, which also takes into account the proportional expansion of the fullerene as the number of absorbed calcium atoms increases. However, the stability of a fullerene system during calcium adsorption also strongly depends on whether any atoms or molecules are being encapsulated by the fullerene, as these encapsulated atoms/molecules can also interact with the fullerene and influence its stability. A Mulliken electronegativity analysis revealed that, when atoms inside and/or outside the fullerene donate charge (electrons) to the fullerene, the fullerene expands. The excess charge on the carbon atoms of the fullerene weakens some of the carbon–carbon bonds, potentially causing them to break, in which case the fullerene loses its ability to encapsulate molecules and releases them.

Keywords Buckyball · C_{60} · Endofullerene · Nanocapsule · Sodium radioiodide

Introduction

Over the past decade, considerable progress has been made in the synthesis and applications of carbon nanotubes and fullerenes [1], as well as other nanoscale systems, in many fields of technology [2, 3]. Indeed, the development of different methods of manipulating matter at the atomic scale [4] has given rise to molecular architecture, as predicted by Feynman [5], which will hopefully solve a great number of problems [6–9] by facilitating the use of quantum-level systems that allow us to take advantage of exclusively nanoscale properties [10].

A cancer is a disease that attacks the body at the cellular level. Cancer has the greatest impact globally of any disease [11], so there is much hope that nanotechnology can be applied in novel ways to help cure cancers, such as in malignant tumor treatments based on the use of functionalized nanoparticles [12, 13]. Although there is still no drug or method that can accurately distinguish cancer cells from healthy ones, such a drug or method could potentially be used to selectively destroy cancer cells while leaving healthy cells unaffected. This would represent a major breakthrough in efforts to minimize the side effects caused by chemotherapy, radiotherapy, and surgical intervention [14].

Following a great deal of statistical research and clinical work on their efficacy and safety, medications have been

✉ Alejandro Valderrama
alecvald@ciencias.unam.mx

[1] Facultad de Ciencias, Universidad Nacional Autónoma de México, Avenida Universidad No. 3000, Ciudad Universitaria, Delegación Coyoacán, C. P. 04510. Ciudad de México, México

successfully applied in many cases to treat diseases leading to abnormal growth of the thyroid gland. Such medications supply various radioiodine compounds such as sodium iodide ($Na^{131}I$) [15, 16], as the high affinity of iodine for the thyroid gland means that the thyroid is able to capture the ^{131}I when it is circulating in the bloodstream. This is also advantageous because it means that the amount of radioiodine captured by the thyroid is proportional to the amount of thyroid tissue present—as the thyroid enlarges it captures more radioiodine and is therefore exposed to more radiation.

Since we now have detailed protocols [17] for using radioactive iodine compounds as medications, it would also be desirable to use them in other body organs that present neoplasms. One possible way to do this is to use nanocapsules, which are endohedral fullerenes (endofullerenes) that encapsulate additional atoms, ions, or clusters. Such nanocapsules could be directed to different tissues in the body to allow the localized delivery of drugs.

In recent studies, thermally sealed single-walled carbon nanotubes (SWNTs) containing certain radioiodine molecules [18] were used as multifunctional transport systems in vivo [19], and it was found that merely encapsulating the iodine compounds in these carbon nanotubes was sufficient to nullify the natural affinity of the radioiodine for the thyroid gland. However, other studies have shown that carbon nanotubes may also have some toxicity in the body, depending upon their dimensions [20, 21]. To overcome this problem, and considering that some of the properties of buckyballs also apply to nanotubes, it seems logical to only consider smaller nanotubes, i.e., endohedral compounds consisting of fullerenes containing different dopants, for use as transport systems. The outer surfaces of these doped fullerenes may also be decorated with other atoms or simple compounds that serve as molecular recognition functions.

However, it is important to gain a better understanding of the properties of these nanocapsules, because a series of studies have demonstrated that the stability of doped fullerenes decreases rapidly with the number of dopant atoms [22]. In a previously published study [23], we found that fullerenes have a good capacity to encapsulate or protect several sodium radioiodide molecules ($Na^{131}I$). However, even though electropotential maps show that the outer and inner fullerene surfaces are almost neutral, the valence of each fullerene carbon atom implies that these atoms are reactive to some degree. As the fullerene is filled, the distances between carbon atoms of the fullerene and the molecules contained therein are reduced with electronic displacements of the iodine atoms towards the carbons which weakens their covalent bonds. Thus, no more than three molecules of $Na^{131}I$ can be encapsulated by a C_{60} fullerene without destabilizing the system. There are also corresponding limits for similar encapsulated molecules such as potassium iodide ($K^{131}I$; limit of two per fullerene) and simple diatomic radioiodine ($^{131}I_2$; the limit is three molecules without breaking the fullerene).

However, as we have shown in recent work [24], the surface or shell of a C_{60} fullerene that is doped may be critically weakened by the displacement of charge from the encapsulated molecules, meaning that its ability to adsorb atoms that act as molecular recognizers on its surface may be restricted. It is therefore necessary to study the physisorption properties of the surface of a fullerene to determine the conditions required for its stability and for it to function as intended. In other words, we need to ensure that endohedral fullerenes are sufficiently stable to permit their use as multifunctional carriers by checking that their cohesion energies are large enough to hold the endohedrally doped fullerene structure together even when the fullerene interacts with external atoms or molecules.

Thus, in the work reported in the present paper, we employed density functional theory (DFT) to explore how the stabilities of fullerenes with and without dopant molecules change as they adsorb increasing numbers of calcium atoms on their outer surfaces. A coating of calcium on the fullerene surface may facilitate molecular recognition by bone tissue via the metabolic cycle. Other studies have used first-principles methods to show that calcium, phosphorus, and strontium atoms can be strongly physisorbed at fullerene surfaces via charge redistribution mechanisms [25]. In this study, we were able to show that the stability and integrity of an endohedral fullerene "nanocapsule" depends on the balance between the cohesive strength of the fullerene structure and the strength of rupturing forces resulting from the expansion of the fullerene framework due to interactions of the fullerene with (i) atoms adsorbed on its outer surface and (ii) dopant molecules encapsulated by the fullerene.

Methods

The methodology that we used to study the endofullerene systems of interest included standard simulations based on geometric optimization (GO) and molecular dynamics (MD), performed mainly using the parallel-processing code Quantum Espresso (version 5.0.2) [26], running pw.x in the self-consistent mode (PWscf). Density functional theory (DFT) [27, 28] was also employed, along with the Born–Oppenheimer approximation, the Martins–Troullier method [29, 30] for generating efficient norm-conserving pseudopotentials (PPs) for use with a plane-wave (PW) basis set to describe electron–ion interactions, and the Perdew–Burke–Ernzerhof (PBE) exchange–correlation functional [31].

Since the molecular systems we studied are finite, in order to integrate the Brillouin zone in the electronic structure calculations, we implemented supercells with a grid of four irreducible *k*-points, and used the Methfessel and Paxton method

of approximating the occupation function [32]. A smearing width of 0.07 eV was applied to obtain faster convergence and offsets in the three directions. The threshold energy convergence was taken to be 0.1 meV. All calculations of the total energy and electronic structure were performed with an estimated SCF accuracy of $<9.0 \times 10^{-5}$ eV. This set of parameters has been shown to be very effective for studying surface-adsorption systems [33, 34]. Additionally, for all of the systems studied, we performed scalar relativistic spin-polarized and non-spin-polarized calculations; since we obtained identical results for both calculations, we were able to verify that these systems are not magnetic.

For all of the molecular systems covered in this study, we performed an analysis of the Mulliken charge distribution, which is obtained by summing the number of electrons in the atomic orbitals associated with a particular atom and then subtracting the positive charge at the core of the atom. To do this, we used the Amsterdam Density Functional (ADF) software running in the Single Point RunType execution mode, which uses a frozen molecular configuration and partitions the total charge density and the total orbital density in order to assign an overlap population to each atom [35]. The energies of the structures were computed based on the valence electronic states for the atoms (carbon: $2s^2 2p^2$, iodine: $5s^2 5p^5$, sodium: $2s^2 2p^6 3s$, calcium: $3s^2 3p^6 4s^2$). The cutoff energy was 544.22 eV.

To calculate the formation energies of fullerene C_{60} with various atoms or molecules inside and some atoms decorating its surface, we considered the difference between the total energy and the sum of the energies of each part:

$$E_f = E\left(n\mathrm{Na}^{131}\mathrm{I}@\mathrm{C}_{60} + m\mathrm{Ca}\right) - \left[60E(\mathrm{C}) + nE\left(\mathrm{Na}^{131}\mathrm{I}\right) + mE(\mathrm{Ca})\right],$$

where $E(n\mathrm{Na}^{131}\mathrm{I}@\mathrm{C}_{60} + m\mathrm{Ca})$ is the energy of the final optimized configuration of the composite system and $[60E(\mathrm{C}) + nE(\mathrm{Na}^{131}\mathrm{I}) + mE(\mathrm{Ca})]$ is the energy of 60 non-interacting gaseous carbon atoms plus the energy of n isolated molecules of $\mathrm{Na}^{131}\mathrm{I}$ and m atoms of Ca. When $n = 0$ and $m = 0$, this equation yields the formation energy of the undecorated and undoped C_{60} fullerene, with an average binding energy per atom of $E_f/60$. Using this simple formula, we were able to calculate the correct cohesive energy per carbon atom in the fullerene.

All of the graphical representations shown in this paper were created with the Scientific Computing & Modelling ADF (release 2009.01) software.

External surface interactions with C_{60} fullerenes

Due their mechanical and electronic properties, and because they are chemically inert molecules, fullerenes and nanotubes are good candidates for potential molecular transporters or functionalized nanocapsules that can travel around the human body to deliver a drug to a particular area of tissue. Therefore, in addition to their interest in determining the abilities of fullerenes to encapsulate various atoms and small molecules [36, 37], some researchers have recently presented studies of the possible interactions of C_{60} fullerene with its environment, such as surrounding water molecules [38, 39]. Simulations have shown that interactions between the carbon atoms of fullerenes and water molecules are rather hydrophobic, even when the fullerene is in a solution of NaCl or KCl [40].

Inside the human body, the solvent through which the functionalized fullerenes (nanocapsules) would carry the radioactive dopant is the blood plasma, which is the liquid component of the blood that allows erythrocytes, leukocytes, and all other metabolic substances in the body to be mobile. Since blood plasma is a 90% aqueous medium, it will only rarely interact with the fullerene, given that the surface of the fullerene is electroneutral according to a map of its electrostatic potential; see Fig. 1. A series of concentric spherical equipotentials occur for the fullerene, with a neutral interface occurring at the carbon bonds, which allows the fullerene to encapsulate other atoms or small molecules because the surface of the fullerene can isolate its interior.

The carbon atoms in the fullerene have an electron configuration of $1s^2 2s^2 2p^2$, and thus present a valence of four. They therefore form hybrid covalent bonds with three other atoms in the structure as well as a nonlocalized π-bond. The electron cloud is distributed symmetrically around each carbon, but there is still a half-empty π-bond on each that is capable of establishing "polar" interactions via van der Waals forces with other atoms or molecules.

It would be useful to know how a C_{60} fullerene physisorbs atoms on its outer surface. Such physisorption occurs when atoms interact with fullerene carbon atoms through a strong mutual polar attraction without any changes of chemical

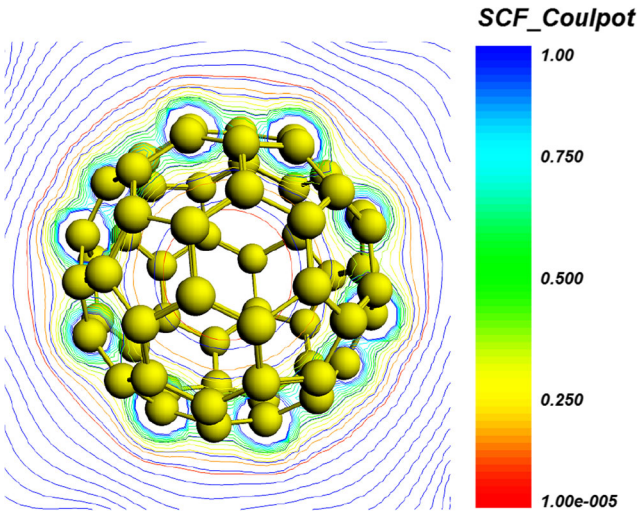

Fig. 1 Electrostatic potential map of a C_{60} fullerene. The scale is normalized, and the almost electroneutral region is shown in *green*

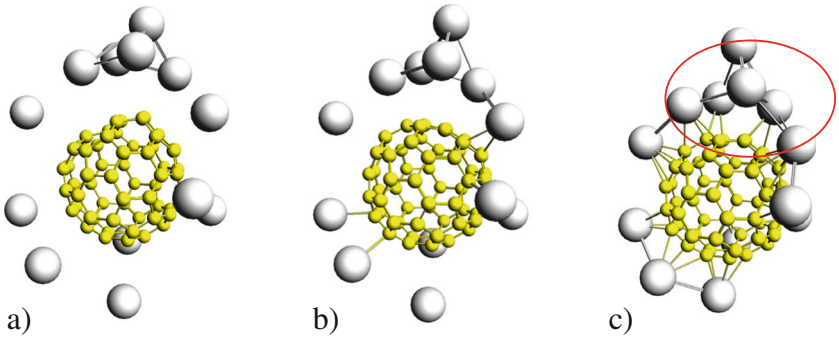

Fig. 2 **a–c** Simulation of a fullerene immersed in a gas of calcium atoms. **a** Representation of the calcium atoms when they are in the vicinity of the fullerene but have not interacted with it yet. **b** Representation of the calcium atoms as they approach the fullerene. **c** Representation of the calcium atoms as they interact with the fullerene, with some of them agglomerating on the surface (these atoms are indicated by the *red oval*)

configuration in the atoms involved in the interaction. That is, none of the carbon atoms of the fullerene are substituted; the other atoms simply "decorate" the fullerene surface. Physisorption is especially important to consider when designing fullerenes for use as functionalized nanocapsules. The functionalization of a nanocapsule is achieved by decorating its outer surface with atoms or molecules that could act as molecular recognizers due to chemical affinity with a particular tissue, meaning that the nanocapsule interacts specifically with that tissue. Atoms of calcium, phosphorus, and strontium [41, 42] can be used as possible molecular recognizers for bone tissue, given their well-known affinities for such tissue. However, the nanocapsule must make its way through the bloodstream without interacting with any of the substances present in the blood to a degree that causes the nanocapsule to release its contents. The nanocapsule must therefore be sufficiently robust to reach its target.

C_{60} fullerene interactions with calcium

When calcium atoms (electron configuration: [Ar]$4s^2$) approach C_{60} sufficiently closely, a van der Waals interaction caused by weak forces resulting from polar redistributions of electron clouds can occur which induces the Ca atoms to adhere to the surface of the fullerene. If the C_{60} maintains its integrity (i.e., it does not fissure and is not disrupted), it is unlikely that the fullerene carbon atoms will bond to the localized electrons of the calcium atoms. This weak attraction

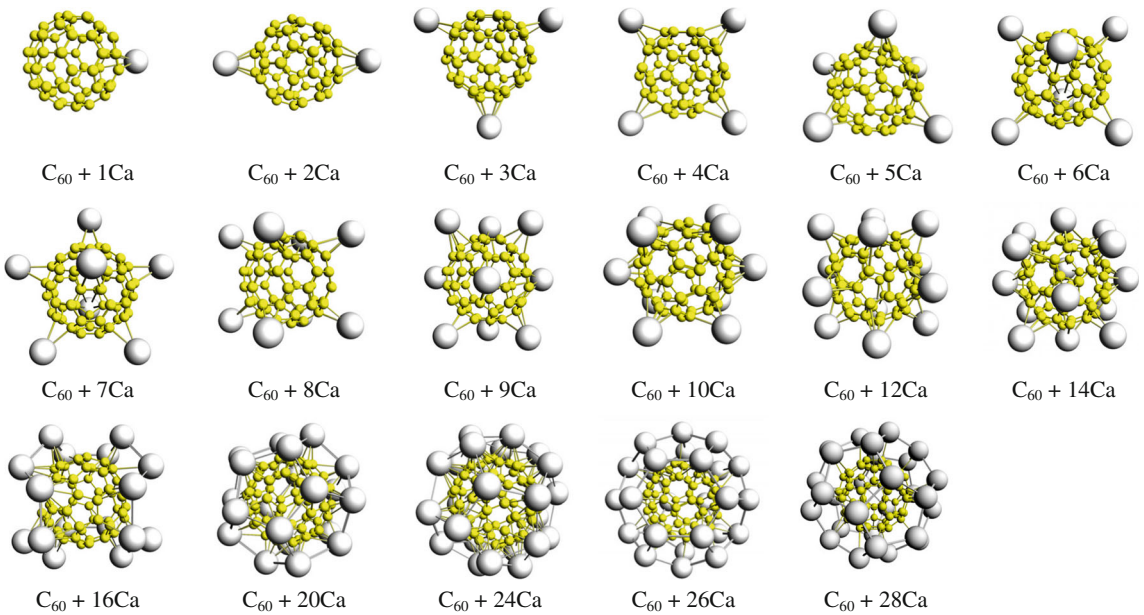

Fig. 3 Initial positions of calcium atoms in the vicinity of fullerene when performing geometric optimization and determining the capacity of the surface of C_{60} to adsorb various numbers of calcium atoms. The number of calcium atoms increases with each new diagram, such that the first diagram contains one calcium atom and the final diagram has 28 calcium atoms. When at least five calcium atoms were present in the simulation, only groups in which the calcium atoms were equidistant were considered; this was achieved by positioning the calcium atoms at the vertices of a convex polyhedron centered on the fullerene, resulting in simulations that included either 1, 2, 3, 4, 5, 6, 7, 8, 9, 10, 12, 14, 16, 20, 24, 26, or 28 calcium atoms

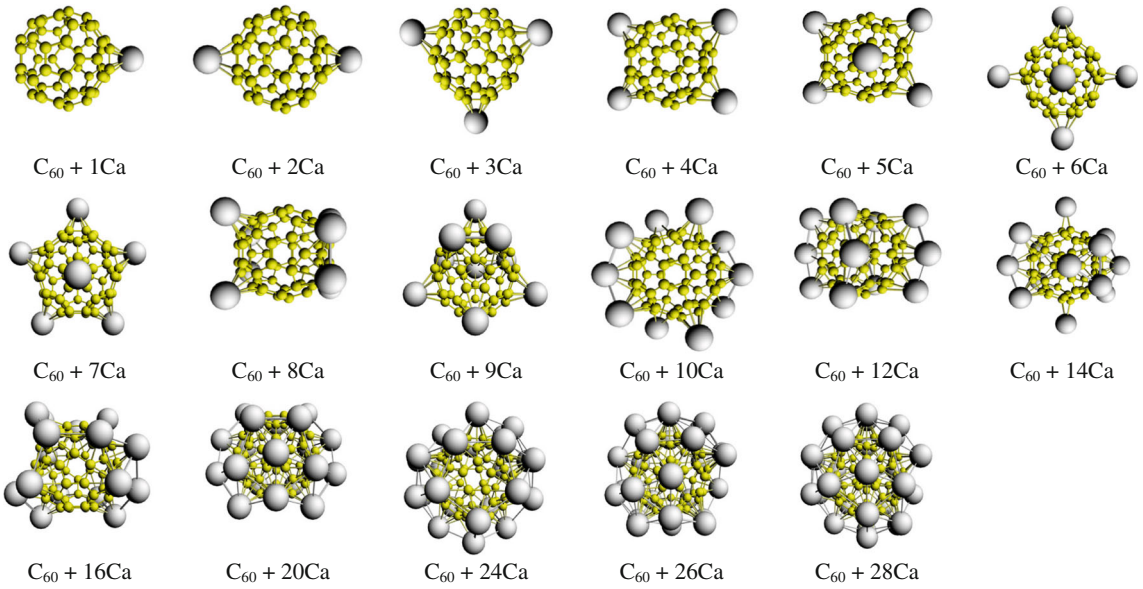

Fig. 4 Positions of the calcium atoms shown in Fig. 3 at the end of the simulation

caused by polar rearrangements of electron clouds is similar to that seen between various atoms, particularly calcium [43], and a graphene sheet. In the present case, however, the geometry is spherical instead of planar.

Interactions between fullerenes and calcium atoms can be studied in different ways. The ability of the fullerene surface to physisorb calcium atoms can be explored via simulation for either a realistic or an idealized situation [44].

Case 1: empirical model

Molecular dynamics simulation of the exposure of C_{60} to a calcium gas in close proximity to its surface indicates that some of the calcium atoms randomly attach to the fullerene when they come into contact with it, as shown in Fig. 2.

As more and more calcium atoms are added to the system, the calcium atoms begin to agglomerate, meaning that some of them lose contact with the surface of the nanocapsule. However, using this procedure, there is no way to determine the limit on the number of calcium atoms that can be physisorbed on the surface of the fullerene. It only allows us to gauge the qualitative response of fullerene to calcium atom physisorption, which depends strongly on the initial random spatial arrangement of the calcium atoms.

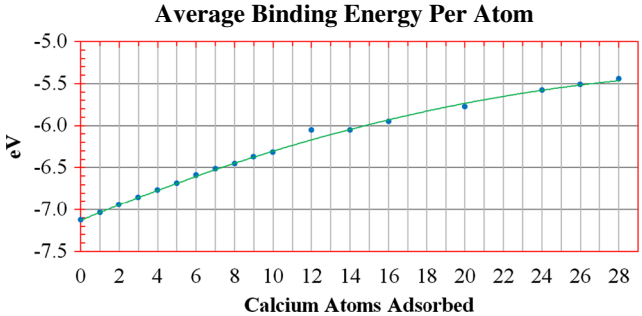

Fig. 5 Average binding energy per atom in the $C_{60} + mCa$ systems. As the system becomes saturated with calcium atoms, the bonds between the atoms weaken

Table 1 Geometric optimization of the composite systems $C_{60} + mCa$, $m \in \{1, 2, 3, 4, 5, 6, 7, 8, 9, 10, 12, 14, 16, 20, 24, 26, 28\}$; E_T is the total energy, E_f is the formation energy, $\langle E_A \rangle$ is the average energy per atom, and $\langle d(C{-}C) \rangle$ is the average length of a fullerene C–C bond

m	E_T (keV)	E_f (eV)	$\langle E_A \rangle$ (eV)	$\langle d(C{-}C) \rangle$ (Å)
0	– 9.279	– 427.59	– 7.13	1.4387
1	– 10.295	– 429.32	– 7.04	1.4404
2	– 11.311	– 430.82	– 6.95	1.4416
3	– 12.327	– 432.23	– 6.86	1.4429
4	– 13.343	– 433.42	– 6.77	1.4438
5	– 14.359	– 434.72	– 6.69	1.4446
6	– 15.375	– 435.34	– 6.60	1.4454
7	– 16.391	– 436.95	– 6.52	1.4467
8	– 17.408	– 439.22	– 6.46	1.4472
9	– 18.423	– 433.14	– 6.28	1.4487
10	– 19.440	– 430.28	– 6.15	1.4475
12	– 21.473	– 436.34	– 6.06	1.4497
14	– 23.505	– 448.25	– 6.06	1.4515
16	– 25.539	– 452.71	– 5.96	1.4545
20	– 29.607	– 462.52	– 5.78	1.4572
24	– 33.673	– 469.00	– 5.58	1.4602
26	– 35.707	– 474.23	– 5.51	1.4611
28	– 37.742	– 479.38	– 5.45	1.4620

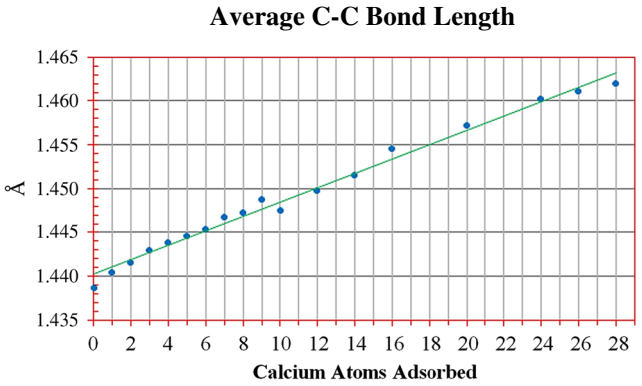

Fig. 6 Average length of a C–C bond in each C_{60} + *m*Ca system. The *green line* shows that the expansion of the fullerene is a linear function of the number of adsorbed Ca atoms

Case 2: geometric model

To overcome the problem of calcium atom agglomeration and overlap, and to more precisely determine the ability of the fullerene to adsorb these atoms, we applied a geometric method in molecular dynamics simulation.

As shown in Fig. 3, we simulated calcium atoms approaching the fullerene such that the initial positions of the calcium atoms were practically equidistant from the center and were always the greatest possible distances from each other. When five and more calcium atoms were simulated, their positions corresponded to the positions of the vertices of a convex polyhedron that was centered on the fullerene and a reasonable distance (2.50–3.00 Å) from its surface, so as to allow interactions between the calcium atoms and fullerene.

Additionally, only groups of calcium atoms arranged in a convex polyhedron where the distances between vertices were at least as large as the average length of a Ca–Ca bond (<*d*(Ca−Ca)> = 3.394 Å) were considered as might occur in convex, polyhedrons with more vertices would be larger and the calcium atoms would move away much from the surface of the fullerene, losing the interaction.

All of the above initial geometric configurations underwent optimization, which yielded the final positions shown in Fig. 4. The systems (i.e., fullerene and the calcium atoms) were very consistent in the sense that the fullerene always adsorbed all of the available calcium. The final (fixed) positions of the calcium atoms were almost the same as their initial positions, although some calcium atoms showed slight shifts or readjustments before they fixed their positions.

Increasing the number of calcium atoms near the fullerene beyond 28 while constraining the atoms to be equidistant from each other meant that the atoms were initially positioned too far from the fullerene surface to allow molecular interactions to occur, making it considerably more difficult for the fullerene to adsorb this many calcium atoms without them overlapping and losing contact with C_{60}.

Based on the symmetry requirements described above, we were able to calculate from the molecular dynamics simulations of the composite systems that increasing the number of calcium atoms adsorbed leads to a proportional decrease in the total energy of the system. However, the average binding energy per atom became less negative as the number of adsorbed atoms was increased, as shown in Fig. 5.

Table 1 shows the values calculated during geometric optimization for the ground states of the simulated systems. It shows values for the total energy, formation energy, and average energy per atom in each system, as well as the average length of a fullerene C–C bond. Each adsorbed calcium atom contributes practically the same formation energy, approximately 1016 eV, which explains the linear decrease in the total energy of the system as more calcium atoms are adsorbed. It is interesting to note that each time the fullerene adsorbs an extra calcium atom it expands slightly, as indicated by the gradual increase in the values in the last column of the table (which lists the average C–C bond length, including both single and double bonds). Figure 6 depicts this trend graphically. To find the reason for this expansion (which is about 2% in the case in which the fullerene is coated with 28 calcium atoms), we performed a Mulliken charge distribution analysis, as described in the next section.

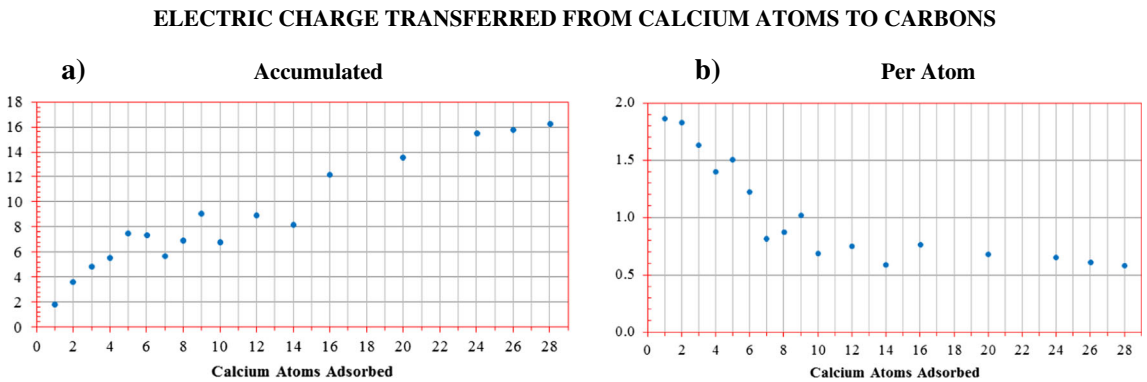

Fig. 7 **a** Total amount of charge transferred from the calcium atoms in various fullerene C_{60} + *m*Ca systems. **b** Average of amount of charge transferred by each calcium atom to the fullerene. Note that both *y*-axes are normalized

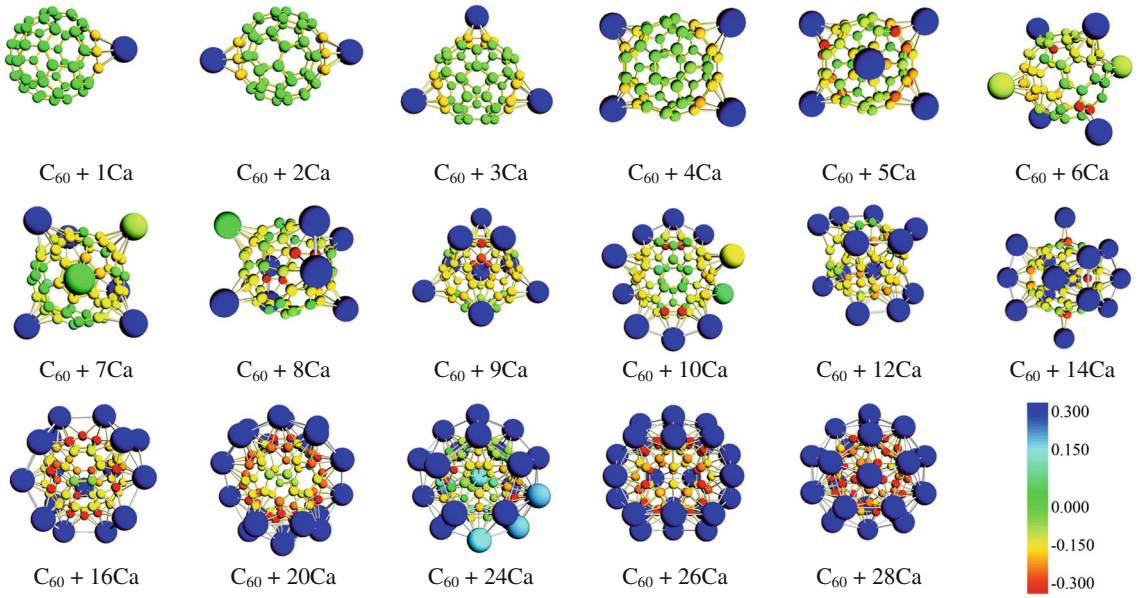

Fig. 8 Mulliken electronegativity distributions in the $C_{60} + mCa$ systems

Mulliken analysis

According to DFT, the electron cloud associated with fullerene C_{60} is redistributed in the presence of calcium atoms (or other species). Using the linear combination of atomic and molecular orbitals method, we examined the Mulliken electronegativities of the $C_{60} + mCa$ systems in order to determine the charge exchange between the calcium atoms and the fullerene carbons.

The fullerene can initially be considered neutral. The polar interaction of a calcium atom with a fullerene carbon results in the calcium passing a small fraction of its valence charge to the carbon atom. The first calcium atoms to be adsorbed pass more of their valence charge to carbon atoms than subsequently adsorbed calcium atoms do. As more and more calcium atoms are adsorbed, the system eventually becomes saturated (see Fig. 7).

The charge transferred to the fullerene by each calcium atom in the $C_{60} + mCa$ system modifies the electronegativities of the carbons closest to each calcium atom. The 4*s* orbital of calcium has sufficient energy to donate a fraction of its charge to a carbon atom. The sequence of calcium atom absorption shown in Fig. 8 depicts the Mulliken charge in each $C_{60} + mCa$ system using a color scale ranging from blue (positive) to red (negative).

Since the calcium atoms donate charge to the fullerene carbons, the carbons accumulate excess charge, resulting in increased repulsion between them, which explains the gradual expansion of the structure with increasing Ca adsorption. However, for the sequence shown in Fig. 8, the expansion is relatively small, so none of the fullerene's bonds are broken and it does not show any noticeable cracks or breaks with increasing adsorption; it maintains its integrity.

Having elucidated that C_{60} can stably adsorb many atoms of calcium when it is empty (i.e., it is not encapsulating any atoms or molecules), the next step was to investigate how this ability changes when some radioactive iodine (^{131}I) molecules are inserted into the nanocapsule, thus producing a functionalized system consisting of a fullerene that contains a radioactive molecule and is decorated with calcium atoms to facilitate the deposition of the fullerene in bone tissue.

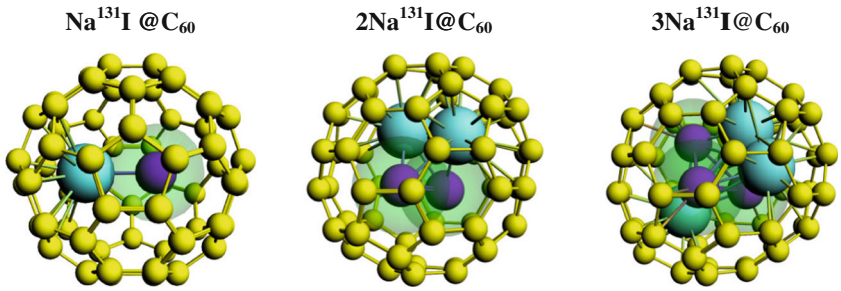

Fig. 9 Endofullerenes containing sodium radioiodide molecules (nNaI@C_{60} where $n = 1, 2, 3$)

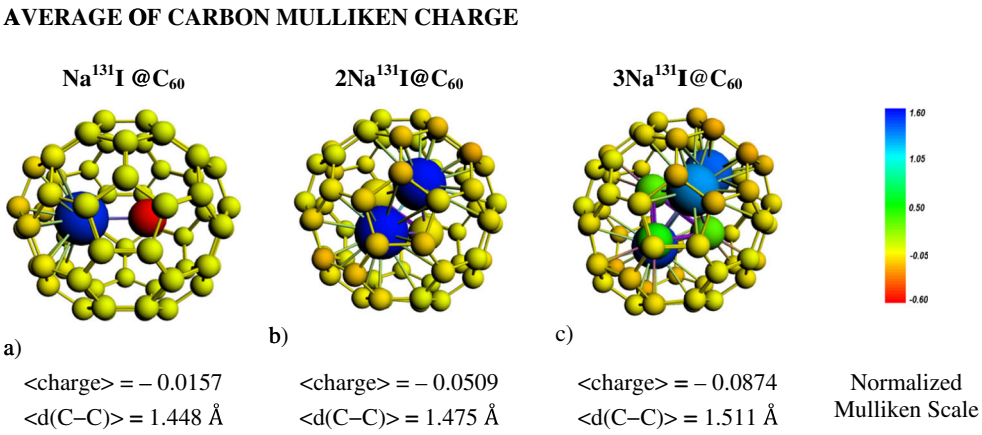

Fig. 10 Mulliken charge distributions on C_{60} fullerenes containing one, two, and three $Na^{131}I$ molecules. Increasing the charge on the fullerene carbons increases the average lengths of the C–C bonds

Interactions of a sodium-radioiodide-containing nanocapsule with calcium

To examine the response of a filled nanocapsule when it interacts with calcium atoms, we considered fullerenes containing some sodium radioiodide molecules, i.e., $n Na^{131}I@C_{60}$ with $n = 1, 2, 3$, as shown in Fig. 9. Note that each iodine atom inserted into the fullerene donates charge to the fullerene carbon, as shown by a Mulliken analysis (see Fig. 10), which leads to excess charge on those carbon atoms. When $n \geq 4$, the excess charge on the carbons is so large that it results in sufficiently strong repulsion between the carbons to break some of the C–C bonds in the fullerene, disrupting its structure [22]. This also means that the structure of the $3NaI@C_{60}$ system is easily broken because the fullerene is full [23].

We therefore simulated a process of successive adsorption of Ca atoms analogous to that previously considered for the empty fullerene, and adhered to the same geometric model. As shown in Fig. 11, the $NaI@C_{60}$ system begins to show cracks in the fullerene structure when more than 14 calcium atoms are adsorbed, while the nanocapsule $2NaI@C_{60}$ begins to crack with the adsorption of the second Ca atom and the structure is disrupted upon the addition of the eighth Ca atom, while the system with three molecules of $Na^{131}I$ breaks apart when it interacts with just one calcium atom (the strength of the interactions of the fullerene with the atoms and molecules inside and outside it exceed the cohesion of the fullerene structure), thus leading to the release of its contents.

Because the $3NaI@C_{60}$ nanocapsule cannot withstand interacting with even a single calcium atom, we could not evaluate the calcium adsorption energy at the fullerene surface (the structure loses its integrity when interacting with a Ca atom, meaning that it is no longer a nanocapsule—its inner and outer properties change). For this reason, we only present the results for the $NaI@C_{60}$ and $2NaI@C_{60}$ systems here.

Table 2 shows the results for the total energy, formation energy, and bonding energy per atom for the $NaI@C_{60}$ and $2NaI@C_{60}$ systems. As can be seen from this table, the behavior of these filled fullerenes upon successive physisorptions of Ca atoms is very similar to the behavior of the empty fullerene during successive adsorptions; the filled fullerenes are both capable of adsorbing all of the calcium atoms in their neighborhood. Nevertheless, the total energy of each system becomes more negative each time a calcium

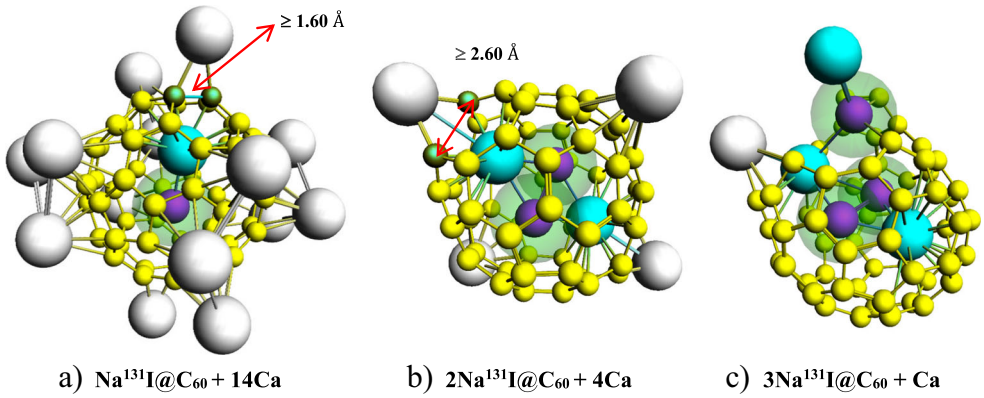

Fig. 11 **a–c** Critical interactions of filled nanocapsules with calcium atoms. **a** The $NaI@C_{60}$ + 14Ca system shows some cracks due to bond lengths ≥ 1.60 Å. **b** The $2NaI@C_{60}$ system presents several disruption points where distances between neighboring carbons are ≥ 2.60 Å. **c** The nanocapsule $3NaI@C_{60}$ breaks completely upon interacting with just one Ca atom, releasing the contents of the fullerene

Table 2 Geometric optimization of the composite systems nNaI@C_{60} + mCa for n = 1, 2, 3 and $m \in \{1, 2, 3, 4, 5, 6, 7, 8, 9, 10, 12, 14, 16, 20, 24, 26, 28\}$; E_T is the total energy, E_f is the formation energy, and $<E_A>$ is the bonding energy per atom

m	NaI@C_{60} + mCa			2NaI@C_{60} + mCa		
	E_T (keV)	E_f (eV)	$<E_A>$ (eV)	E_T (keV)	E_f (eV)	$<E_A>$ (eV)
0	−9.600	−423.03	−6.82	−9.911	−407.19	−6.36
1	−10.617	−425.22	−6.75	−10.928	−409.60	−6.50
2	−11.633	−426.59	−6.67	−11.944	−411.16	−6.42
3	−12.650	−428.27	−6.59	−12.961	−413.18	−6.36
4	−13.666	−429.44	−6.51	−13.976	−413.62	−6.27
5	−14.682	−431.00	−6.43	−14.992	−415.01	−6.19
6	−15.697	−431.80	−6.35	−16.009	−416.83	−6.13
7	−16.714	−433.42	−6.28	−17.025	−418.45	−6.06
8	−17.730	−435.34	−6.22	−18.042	−420.59	−6.01
9	−18.746	−436.65	−6.15	−19.058	−421.72	−5.94
10	−19.763	−438.87	−6.10	−20.075	−424.01	−5.89
12	−21.796	−442.14	−5.97	−22.106	−426.46	−5.76
14	−23.828	−444.79	−5.85	−24.141	−431.67	−5.68
16	−25.861	−448.62	−5.75	−26.175	−436.37	−5.59
20	−29.930	−459.08	−5.60	−30.241	−443.48	−5.41
24	−33.996	−465.86	−5.42	−34.308	−451.77	−5.25
26	−36.021	−462.01	−5.25	−36.351	−465.82	−5.29
28	−38.066	−477.64	−5.31	−38.382	−466.49	−5.18

atom is added, and the binding energy per atom decreases as each system becomes saturated with calcium, as shown in Fig. 12. This reveals that these systems become less stable as the number of adsorbed calcium atoms increases.

Table 3 shows the average length of a C–C bond in the NaI@C_{60} and 2NaI@C_{60} systems, as well as the maximum distance between connected carbon atoms in the structure of each endofullerene. The table indicates that the average length of a carbon bond is always ≤1.54 Å, which is the length of a C–C bond in diamond, and can be assumed to be the maximum length of an ordinary covalent C–C bond. However, while these structures are stable, they do show maximum distances between connected carbon atoms of ≥1.60 Å

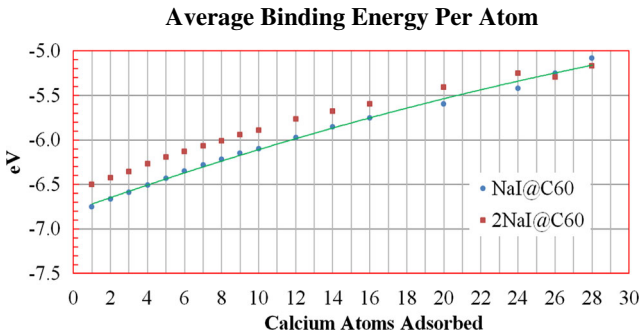

Fig. 12 Average binding energy per atom in each nNaI@C_{60} + mCa system

Table 3 Fullerene carbon bond lengths in the composite systems nNaI@C_{60} + mCa for n = 1, 2, 3 and $m \in \{1, 2, 3, 4, 5, 6, 7, 8, 9, 10, 12, 14, 16, 20, 24, 26, 28\}$; $<d(C-C)>$ is the average length of a C–C bond in the fullerene, whereas $<d_M(C-C)>$ is the maximum distance between connected carbon atoms in the fullerene

m	NaI@C_{60} + mCa		2NaI@C_{60} + mCa	
	$<d(C-C)>$ (Å)	$<d_M(C-C)>$ (Å)	$<d(C-C)>$ (Å)	$<d_M(C-C)>$ (Å)
0	1.4482	1.5000	1.4751	1.5327
1	1.4496	1.4990	1.4767	1.5475
2	1.4508	1.4974	1.4785	*1.6017*
3	1.4524	1.5353	1.4810	*1.6860*
4	1.4531	1.4964	1.4972	***2.6805***
5	1.4543	1.5082	1.4978	***2.3973***
6	1.4553	1.6149	1.4833	*1.6170*
7	1.4564	1.5321	1.4848	*1.6274*
8	1.4562	1.5020	1.4852	***1.7034***
9	1.4587	1.5320	1.4891	***1.8388***
10	1.4571	1.5269	1.4877	***1.7009***
12	1.4594	1.5276	1.5066	***2.3916***
14	1.4614	*1.6086*	1.4941	***1.6876***
16	1.4639	*1.5999*	1.4950	***1.6553***
20	1.4670	*1.5692*	1.4965	***1.6498***
24	1.4702	*1.5747*	1.5002	***1.6469***
26	1.4709	*1.5812*	1.5026	***1.7204***
28	1.4715	*1.5802*	1.5076	***1.7555***

(corresponding to fissures in the fullerene structure) when a certain number of calcium atoms have been adsorbed (these distances are italicized in the table). Indeed, some of the maximum distances between connected carbon atoms are ≥1.70 Å, and these correspond to disruption points in the structure (these distances are highlighted in bold italics in the table).

Conclusions

As we have seen in this work, fullerenes have the ability to adsorb many calcium atoms on their surfaces. When calcium atoms are physisorbed on a fullerene surface by weak van der Waals forces, they transfer some of their valence electronic charge to the fullerene, weakening the carbon–carbon bonds and causing the structure to expand by up to 3% in size in the Ca-saturated case (a maximum of 28 calcium atoms can be adsorbed onto the surface of the fullerene while maintaining its structural integrity).

However, when a fullerene is initially doped with radioiodine molecules (which transfer a fraction of their electronic charge to the carbon–carbon bonds of the fullerene), the capacity of the fullerene to absorb calcium atoms without affecting its structure decreases. Thus, during the adsorption

of Ca atoms, doped fullerene systems soon become oversaturated and exceed their limit of expandability, leading to cracks and breaks in the fullerene and even a total loss of its ability to encapsulate molecules. Similar behavior can be expected with other dopant molecules, such as potassium radioiodide $K^{131}I$ and molecular radioiodine $^{131}I_2$, and with other atoms that decorate the fullerene, such as phosphorus and strontium (known for their affinity for bone tissue).

In short, simple fullerenes are not robust enough to allow the design of nanocapsules with radioactive contents and surface decorations that could potentially be used to fight tumors, as they could easily break during their journey around the bloodstream, releasing their contents before reaching the target tissue. It is therefore necessary to redesign the nanocapsules to be more robust. One way to do this would be to utilize a multilayered fullerene (such as a "nano-onion") in which the action of the dopant in the inner fullerene layer could be separated from the action of the decorating atoms that function as molecular recognizers on the outermost fullerene layer.

Acknowledgements Special thanks to Consejo Nacional de Ciencia y Tecnología for their financial support of this work through the national postdoctoral program, and to the NES-Miztli Supercomputer Center of the Dirección General de Tecnologías de la Información y Comunicación, Universidad Nacional Autónoma de México for their technical support in relation to many of the computations performed.

References

1. Dresselhaus et al. (2008) Carbon nanotubes: advanced topics in the synthesis, structure, properties and applications. Springer, Berlin. ISBN 978-3-540-72865-8. http://www.springer.com/us/book/9783540728641
2. Melnik R (ed) (2012) Nanoscale Syst Math Model Theory Appl 1: 1–186. ISSN: 2299–3290. doi:10.2478/nsmmt-2012-0011. http://www.degruyter.com/view/j/nsmmt
3. Muthukumar M, Plesa C, Dekker C (2015) Single-molecule sensing with nanopores. Physics Today 68:40. doi:10.1063/PT.3.2881.
4. Custance O, Perez R, Morita S (2009) Atomic force microscopy as a tool for atom manipulation. Nature Nanotechnol 4:803–810. doi:10.1038/nnano.2009.347, http://www.nature.com/nnano/journal/v4/n12/abs/nnano.2009.347.html
5. Drexler E (2009) "There's plenty of room at the bottom" (Richard Feynman, Pasadena, 29 December 1959). In: Eric Drexler's blog: Metamodern: The Trajectory of Technology. http://metamodern.com/2009/12/29/theres-plenty-of-room-at-the-bottom%E2%80%9D-feynman-1959/
6. Malsch I (2003) Nanoforum: Nanotechnology helps solve the world's energy problems. http://www.nanotech-now.com/Ineke-Malsch/IMalsch-energy-paper.htm
7. Lindquist E, Mosher-Howe KN, Liu X (2010) Nanotechnology… what is it good for? (absolutely everything): a problem definition approach. Policy Studies Organization, Washington, DC. doi:10.1111/j.1541-1338.2010.00441.x
8. Tang SKY (2011) The nanotechnology solution to the global water challenge. Science in the News (Harvard University) 21 June 2011. http://sitn.hms.harvard.edu/flash/2011/issue95/#respond
9. Salje EKH (2010) Multi-scaling and mesoscopic structures. Philos Trans A Math Phys Eng Sci 368:1163–1174. doi:10.1098/rsta.2009.0266. http://rsta.royalsocietypublishing.org/content/roypta/368/1914/1163.full.pdf
10. Ekinci KL, Roukes ML (2005) Nanoelectromechanical systems. Rev Sci Instrum 76:061101. doi:10.1063/1.1927327, http://nano.caltech.edu/publications/papers/Ekinci-RSI2005.pdf
11. Stewart BW, Wild CP (2015) World Cancer Report 2014. World Health Organization, Geneva. ISBN 978-92-832-0429-9. http://www.iarc.fr/en/publications/books/wcr/wcr-order.php
12. Yoon HJ et al (2013) Sensitive capture of circulating tumour cells by functionalized graphene oxide nanosheets. Nat Nanotechnol 8: 735–741. doi:10.1038/nnano.2013.194, http://www.nature.com/nnano/journal/v8/n10/full/nnano.2013.194.html
13. Peer D (2007) Nanocarriers as an emerging platform for cancer therapy. Nat Nanotechnol 2:751–760. doi:10.1038/nnano.2007.387, http://www.nature.com/nnano/journal/v2/n12/full/nnano.2007.387.html
14. American Cancer Society, Inc. (2015) Treatments and side effects. http://www.cancer.org/treatment/treatmentsandsideeffects/index
15. Maxon HR 3rd, Smith HS (1990) Radioiodine-131 in the diagnosis and treatment of metastatic well differentiated thyroid cancer. Endocrinol Metab Clin North Am 19:685–718. http://www.ncbi.nlm.nih.gov/pubmed/2261912
16. Jang S et al (2015) Novel analogs targeting histone deacetylase suppress aggressive thyroid cancer cell growth and induce re-differentiation. Cancer Gene Ther 22:410–416. doi:10.1038/cgt.2015.37, http://www.nature.com/cgt/journal/v22/n8/pdf/cgt201537a.pdf
17. Nwatsock JF et al. (2012). Radioiodine thyroid ablation in Graves' hyperthyroidism: merits and pitfalls. World J Nucl Med 11(1):7–11. doi:10.4103/1450-1147.98731, http://www.ncbi.nlm.nih.gov/pmc/articles/PMC3425234/?report=classic
18. Shao L, Tobias G, Huh Y, Green MLH (2006) Reversible filling of single walled carbon nanotubes opened by alkali hydroxides.Carbon 44:2855–2858. http://www.sciencedirect.com/science/article/pii/S0008622306003393
19. Hong SY, Tobias G (2010) Filled glycosylated carbon nanotubes for in vivo radioemitter localization and imaging. Nat Mater 9:485–490. doi:10.1038/nmat2766
20. Kostarelos K (2008) The long and short of carbon nanotube toxicity. Nat Biotechnol 26(7):774–6. doi:10.1038/nbt0708-774, http://www.nature.com/nbt/journal/v26/n7/full/nbt0708-774.html
21. Martinčić M, Pach E, Ballesteros B, Tobias G (2013) Filling of single-walled and multi-walled carbon nanotubes with inorganic payloads. In: Abstract Collection for NanoMedicine School, Trieste, Italy, 10–11 Sept 2013. http://www.dscf.units.it/nms2013/Abstract_files/NMS2013%20Abstract%20collection.pdf
22. Umran NM et al. (2015) Study of endohedral doped C_{60} fullerene using model potentials. Mater Res Express 2:055603. doi:10.1088/2053-1591/2/5/055603, http://iopscience.iop.org/2053-1591/2/5/055603/article
23. Valderrama A, Guzmán J (2014) Encapsulation of sodium radioiodide in fullerene C_{60}. J Mol Model. 20:2130. doi:10.1007/s00894-014-2130-y
24. Valderrama A, Reynoso R, Gómez RW, Marquina V (2016) Self-stability of C_{60} nanocapsules with radio-iodide content and its interaction with calcium atoms. J Mol Model 22:28. doi:10.1007/s00894-015-2898-4.
25. Yoon M et al (2008) Calcium as the superior coating metal in functionalization of carbon fullerenes for high-capacity hydrogen storage. Phys Rev Lett 100:206806. doi:10.1103/PhysRevLett.100.206806
26. Giannozzi P, Baroni S, Bonini N, Calandra M, Car R, Cavazzoni C et al (2009) Quantum ESPRESSO: a modular and open-source software project for quantum simulations of materials. J Phys

Condens Matter 21:395502. http://www.quantum-espresso.org/news/1494/
27. Bickelhaupt FM, Baerends EJ (2007) Kohn–Sham density functional theory: predicting and understanding chemistry. In: Lipkowitz KB, Boyd DB (eds) Reviews in computational chemistry, volume 15. Wiley, Hoboken. doi:10.1002/9780470125922.ch1
28. Lejaeghere K, Bihlmayer G, Björkman T, et al. (2016) Reproducibility in density functional theory calculations of solids. Science 351:1415. doi:10.1126/science.aad3000, http://science.sciencemag.org/content/351/6280/aad3000
29. Troullier N, Martíns JL (1991) Efficient pseudo potentials for plane-wave calculations. Phys Rev B 43:1993–2006. http://www.tddft.org/TDDFT2004/PracticalSessions/papers/troullier_prb43.1993.pdf
30. Giannozzi P (2015) Notes on pseudopotential generation. Universita di Udine/IOM-Democritos, Trieste. http://www.quantum-espresso.org/wp-content/uploads/Doc/pseudo-gen.pdf
31. Paier J et al (2005) The Perdew–Burke–Ernzerhof exchange-correlation functional applied to the G2-1 test set using a plane-wave basis. J Chem Phys 122:234102. doi:10.1063/1.1926272, http://scitation.aip.org/content/aip/journal/jcp/122/23/10.1063/1.1926272
32. Methfessel M, Paxton A (1989) High-precision sampling for Brillouin-zone integration in metals. Phys Rev B 40:3616. doi:10.1103/PhysRevB.40.3616
33. González-Hernández R, López-Pérez W, Moreno-Armenta MG, Rodríguez JA (2010) Vanadium adsorption and incorporation at the GaN(0001) surface: a first-principles study. Phys Rev B 81:195407. https://journals.aps.org/prb/abstract/10.1103/PhysRevB.81.195407
34. Timon V, Brand S, Clark SJ, Abram RA (2005) Theoretical adlayer surface morphology of wurtzite 2×2 reconstructions of the GaN(0001) surface. J Phys Condens Matter 17:17. doi:10.1088/0953-8984/17/1/002
35. Scientific Computing & Modelling NV (2011) ADF program system. Scientific Computing & Modelling NV, Vrije Universiteit, Amsterdam. http://www.scm.com
36. Dolgonos GA, Peslherbe GH (2014). Encapsulation of diatomic molecules in fullerene C60: implications for their main properties. Phys Chem Chem Phys 47:26294–26305. doi:10.1039/C4CP04069D, http://pubs.rsc.org/en/content/articlelanding/2014/cp/c4cp04069d#!divAbstract
37. Tereshchuk P, Da Silva JLF (2012) Encapsulation of small magnetic clusters in fullerene cages: a density functional theory investigation within van der Waals corrections. Phys Rev B 85:195461. doi:10.1103/PhysRevB.85.195461
38. Walther JH, Jaffe R, Halicioglu T, Koumoutsakos P (2001) Carbon nanotubes in water: structural characteristics and energetics. Chem Phys B 105:9980. doi:10.1021/jp011344u
39. Popadić A, Praprotnik M, Koumoutsakos P, Walther JH (2015) Continuum simulations of water flow past fullerene molecules. Eur Phys J Spec Top 224:2321–2330. doi:10.1140/epjst/e2015-02414-y
40. Jaffe RL, Walther JH, Kotsalis E, Werder T, Koumoutsakos P, Halicioglu T (2013) Molecular dynamics simulations of fullerenes and carbon nanotubes in water. NASA Ames Research Center, Moffett Field. http://www.electrochem.org/dl/ma/201/pdfs/0937.pdf
41. Wasserman RH (1998) Strontium as a tracer for calcium in biological and clinical research. Clin Chem 44(3):437–439. http://www.clinchem.org/content/44/3/437.extract
42. Wong CT et al (2004) In vivo cancellous bone remodeling on a strontium-containing hydroxyapatite (Sr-HA) bioactive cement. J Biomed Mater Res A 68A(3):513–521. doi:10.1002/jbm.a.20089
43. Lee H et al. (2010) Calcium-decorated graphene-based nanostructures for hydrogen storage. Nano Lett 10:793–798. doi:10.1021/nl902822s
44. Fernández-Torre D, Kupiainen O, Pyykkö P, Halonen L (2009) Long-range interactions between polar molecules and metallic surfaces: a comparison of classical and density functional theory based models. Chem Phys Lett 471:239–243. http://www.sciencedirect.com/science/article/pii/S0009261409001936